Applied Surface Science 638 (2023) 158072

Contents lists available at ScienceDirect

Applied Surface Science

journal homepage: www.elsevier.com/locate/apsusc

Full Length Article

Nucleation and growth of low resistivity copper thin films on polyimide substrates by low-temperature atomic layer deposition

Zihong Gao [a], Chengli Zhang [c], Junhua Gao [a], Qiang Wang [c], Guanglong Xu [c], Hongtao Cao [a,b], Hongliang Zhang [a,b,*]

[a] Laboratory of Advanced Nano Materials and Devices, Ningbo Institute of Materials Technology and Engineering, Chinese Academy of Sciences, Ningbo 315201, China
[b] Center of Materials Science and Optoelectronics Engineering, University of Chinese Academy of Sciences, Beijing 100049, China
[c] Ningbo Wakan Electronic Science Technology Co. LTD, Ningbo 315475, China

ARTICLE INFO

Keywords:
Low Resistance Copper Thin Films
Polyimide Substrates
Low-Temperature Atomic Layer Deposition
Growth Mechanism

ABSTRACT

The metallization of polyimide (PI) remains a formidable challenge when using an atomic layer deposition of copper. The present study employs $Cu(hfac)_2$ and Et_2Zn to deposit the copper thin films that are highly conformal and continuous, and possess low resistivity (5.6 μΩ·cm), through a low-temperature atomic layer deposition (120 °C) with multi-pulse of $Cu(hfac)_2$ process on a treated polyimide surface. The process exhibited both self-limiting ALD and CVD-like reactions with a growth rate of 0.079 nm/cycle. The findings demonstrate that an increase in functional groups and adsorption area on the surface of treated PI substrates enhances the adsorption of $Cu(hfac)_2$. A model has been developed to describe the nucleation and growth kinetics of atomic layer deposition of copper on polyimide substrates, based on the adsorption mechanism of $Cu(hfac)_2$ and the interface structure of ALD-Cu/treated PI onto the surface and into the near-surface region of the PI substrates. The academic developing in this work provides theoretical and experimental basis for the deposition using other copper precursors onto polymeric substrates in the future.

1. Introduction

Flexible printed circuits (FPC) are the crucial connective parts between chips for realizing functions of information transmission, signal processing, memory and so on. The last decade has seen explosive growth of FPC, such as (organic light-emitting devices) OLEDs, RFID tags, intelligent wearable devices, smart cards and solar cells. Copper, as one of the most attractive conducting materials in FPC, offers more advantages than various kinds of other materials including silver, carbon nanotube and graphene, so it has historically been the dominant interconnect material [1]. Electroless plating is currently more popular than those conventional technologies including inkjet printing, screen printing and transfer printing because of its advantages of low cost, low temperature process and mass production [2,3]. It seems that noble metals like Pt, Pd and Ag or copper nanoparticles are necessary and usually employed as catalyst seeds or copper seeds in electroless plating process for depositing copper wires on the activated surfaces in an electroless plating bath [3]. An example of direct low-temperature deposition of conductive metal layers onto organic surfaces is the utilization of [(1,2,5,6-η)-1,5-hexadiene] dimethylplatinum(II) (HDMP) and O_2 for Pt deposition on fiber surfaces [4]. Obviously, all the previously mentioned noble metals suffer from some serious disadvantages considering interface compatibility and economical cost of FPC. However, issues with existing electroless plating processes limiting their potential applicability include adhesion between copper thin films and flexible substrates, unintentional incorporation of reducing agents and cost of the materials.

In this context, there are several attempts to develop copper seed layer based on atomic layer deposition as a method of manufacturing high-quality thin films and producing tailored molecular structures for conventional substrates including Si, SiO_2, glass et al. For example, low-temperature atomic layer deposition of low-resistivity copper thin films deposited at the low temperature of 120 °C on a Si or glass substrate has been developed to possess a low resistivity of 1.9 μΩ·cm from $Cu(dmap)_2$ (dmap dimethylamino-2-propoxide) in combined with tertiary butyl hydrazine [5]. The ALD technique also uses hydrogen plasma as a key

* Corresponding author at: Laboratory of Advanced Nano Materials and Devices, Ningbo Institute of Materials Technology and Engineering, Chinese Academy of Sciences, Ningbo 315201, China.
E-mail address: zhanghl@nimte.ac.cn (H. Zhang).

https://doi.org/10.1016/j.apsusc.2023.158072
Received 31 May 2023; Received in revised form 7 July 2023; Accepted 17 July 2023
Available online 19 July 2023

enabling tool for preparation temperature miniaturization [6]. The pure, continuous, smooth, and highly conformal Cu thin films on a Si or glass have emerged below 100 °C by employing the highly reactive copper(I)-N,N'-diisopropylacetamidinate precursor along with the H_2 plasma. Recently, a novel ALD process is reported to yield uniform and conformal Cu thin films on a Si substrate at growth temperatures of 100 ~ 120 °C using the ligand-exchange reaction of $Cu(dmap)_2$ with Et_2Zn [7]. The atomic layer deposited copper thin films employed as anode using the same precursors and 'window' (mentioned above) on PET substrates have been promoted to demonstrate improvement in mechanical robustness and fabrication process simplification of organic light-emitting devices [8].

Polyimide is commonly used as a flexible substrate for flexible printed circuits in the electronics industry due to its good thermal stability, chemical stability and high modulus of elasticity [9]. It is still a big challenge to develop continuous, highly conformal and low resistivity copper thin films on polyimide substrates owing to the lack of functional groups, large porosity and free volume on the PI surface. There is still a lack of in-depth studies on the growth of low resistance copper thin films on polyimide substrates by low-temperature atomic layer deposition.

Herein, we describe a process for low-temperature atomic layer deposition of Cu thin films on non-polar polyimide substrates by employing $Cu(hfac)_2$ (copper(II)-hexafluoroacetylacetonate) as the Cu source and Et_2Zn as the reducing agent without any additional buffer layer. Nucleation and growth of the $Cu(hfac)_2 + Et_2Zn$ process can be improved by a continuous $Cu(hfac)_2$ multi-pulse. A possible growth mechanism of copper thin films on polyimide substrates by low-temperature atomic layer deposition has been proposed.

2. Experiment

2.1. Substrate treatment

Different from lab-level cleaning process for conventional rigid substrates (such as Si, SiO_2, Glass and so on), the industry standard pre-treatment process (ISPP) for processing the surface of the PI substrates in FPC mass production was adopted in this case to make the ALD-Cu process easier for industrial systems. Thus, one of the great advantages of the pre-treatment process is its excellent compatibility with the existing industrial processes. The typical scheme for modifying the surface of a commercial FPC substrate was applied to polyimide slices (Kapton 100HN, DuPont). The industry standard pre-treatment process (ISPP) has been listed in Table S1. The process of adhesive-free flexible copper clad laminate can serve as a reference for the commercial hot lamination of Cu foil in the previous work [10]. The ISPP involves a multi-step process including Cu foil etching, roughening in NaOH, neutralization in HCl, and immediately multiple cleaning in absolute alcohol and deionized water. The multiple cleaning process prior to the deposition of ALD-Cu can greatly reduce contamination. XPS results show that the pre-treated PI only exhibits copper-related characteristic peaks compared to the original PI (Figure S1 and Table S2), confirming that the pre-treated PI substrates are almost free of contamination by the industry standard pre-treatment process (ISPP).

2.2. Deposition of Cu thin films

The deposition was performed in a commercial thermal type ALD reactor equipment (TALD-150D, Kemicro) with 6-inch reaction chamber. $Cu(hfac)_2$ and Et_2Zn were used as reaction precursors. $Cu(hfac)_2$ and Et_2Zn with purity of 99.9% made by AimouYuan (Nanjing, China) were evaporated at 90 °C and 25 °C, respectively. N_2 (7 sccm) was served as both the carrier and purging gas for the precursor vapor. The temperature of the pipeline was set to 110 °C to prevent the precursor from condensing in the pipeline. The polyimide substrates were placed in the center of the cavity and maintained at 120 °C during the deposition process. The ALD growth of metallic copper occurs during alternating exposures to $Cu(hfac)_2$ and Et_2Zn. An ALD cycle was consisted of exposing to $Cu(hfac)_2$ for different exposure modes (single-pulse mode: 1×0.5 s, dual-pulse mode: 2×0.5 s and triple-pulse mode: 3×0.5 s) followed by purging with N_2 for 30 s, then exposing to Et_2Zn for 0.02 s followed by purging with N_2 for 30 s (see Figure S2 in supporting information). The Cu thin films were grown at temperatures of 120 °C under a pressure of 0.1 Torr. The base pressure of the ALD system is 0.0056 Torr.

2.3. Characterization of Cu thin films

The polyimide surface modification was evaluated with a water contact angle meter (OCA25, Dataphysics). Atomic force microscope (Dimension, Vecco, Knock mode) was used to scan the polyimide substrates for surface morphology and roughness. AFM images were analyzed using the related image software NANO Scope 2.0. The thickness, surface morphologies of the copper thin films were obtained using a scanning electron microscope (SEM) (Verios G4 UC, Thermo Scientific). Electrical properties of the copper thin films were measured at room temperature using a Hall effect measurement system (HL-5500PC, Nanometrics). The average value of the resistivity is acquired by data acquisition of 3 samples from the same experiment. The obtained results were then corrected using a model of roughness-induced resistivity variation in thin metal films, as proposed by Aniruddha Konar [11]. The surface chemistry of the copper thin film was analyzed by an X-ray spectrometer, X-ray photoelectron spectra (XPS) (Axis Ultra DLD, Kratos) using Al K_α (1486.6 eV) radiation as an X-ray source with a voltage of 15 kV and a power of 120 W at a pressure of $\sim 5 \times 10^{-9}$ Torr. The energy resolution of the energy analyzer at this passing energy is about 0.48 eV. The binding energies of the copper thin film were corrected for surface charging by referencing to adventitious carbon C1s at 284.8 eV. The XPS core level spectra were fitted using a Shirley and linear type background. The film microstructures and elemental analysis of the Cu/PI interface were examined by transmission electron microscopy (TEM) (JEOL, F200) equipped with energy dispersive x-ray analyzer (EDX). Scotch tape tests (Scotch 600-CQ33, 3 M) were used to test the film-based adhesion of the copper thin film and substrate.

3. Results and discussion

3.1. Adsorption of $Cu(hfac)_2$

Fig. 1 shows SEM images of the surface and cross-sectional morphologies of the copper thin films deposited on the surface of treated polyimide substrates by 500 growth cycles with different exposure modes of $Cu(hfac)_2$ precursor. The obtained films enjoy uniform grain size and homogeneous distribution of copper nanoparticles. The adsorption and filling efficiency of the precursor molecules onto the substrate or film surface during deposition is improved by the multi-pulse process [12]. Fine particles of homogeneous and dense copper are presented in the ALD-Cu thin film for $Cu(hfac)_2$ single-pulse mode (Fig. 1a). The grain boundary edges of copper become more predominant by adopting $Cu(hfac)_2$ double-pulse mode, as presented in Fig. 1c. There are larger copper particles (or copper islands) in the ALD-Cu thin film with clear boundary coalesce (Fig. 1e) for $Cu(hfac)_2$ triple-pulse mode. Correspondingly, the area density of copper islands decreases as the number of $Cu(hfac)_2$ pulse increases. Moreover, highly conformal copper layer with a thickness of up to 21.33 nm has been synthesized on rough PI substrates by atomic layer deposition. Interestingly, the thickness of copper thin films increases from 21.33 nm to 39.47 nm with the increase of the number of $Cu(hfac)_2$ pulse, as shown in Fig. 1b, d and f. In other words, the deposition rate of the copper thin films is significantly increased by increasing the number of $Cu(hfac)_2$ precursor (Figure S3). The growth rate of the copper thin film on treated PI in Cu $(hfac)_2$ triple-pulse mode is estimated to be approximately 0.079 nm/

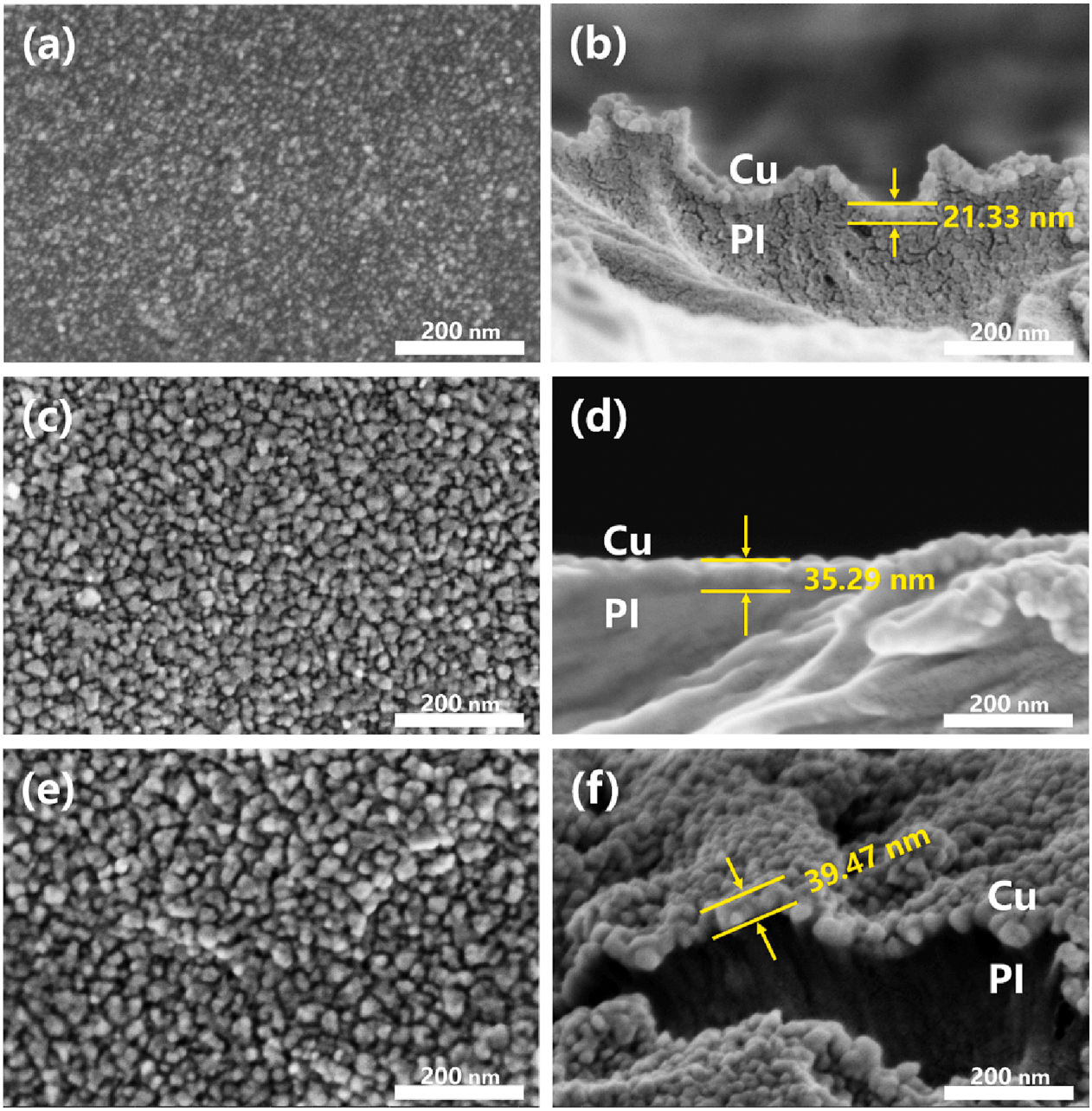

Fig. 1. A comparison between SEM images of the surface and cross-sectional morphologies of the Cu thin films with 500 growth cycles deposited with (a, b) single-pulse mode, (c, d) dual-pulse mode and (e, f) triple-pulse mode on treated PI substrates.

cycle, higher than of ALD-Cu thin film on conventional Si/SiO_2 from single-pulse $Cu(hfac)_2$ [13,14]. In fact, achieving an ideal self-limiting deposition mode for ALD-Cu on polymer surfaces is challenging due to a potential parasitic CVD in ALD processes. The growth rate for single-pulse, double-pulse and triple-pulse experiments is determined to find a balance between parasitic CVD and self-limiting ALD, in order to optimize the process of ALD copper seed layers. The aim is to achieve copper seed layers with uniform thickness and low electrical resistivity that meets general FPC process requirements. It seems to be inferred that the improvement of deposition rate of ALD-Cu thin film can be attributed to the adsorption saturation of $Cu(hfac)_2$ on the PI substrate surface in the triple-pulse mode. As mentioned in the previous literature, the adsorption of Cu precursors has a significant effect on improving the growth rate of atomic layer deposited copper thin films [15]. The resistivity of the copper thin film for dual-pulse mode and triple-pulse mode is measured to be ~ 11.07 mΩ·cm and 33.45 μΩ·cm by Hall measurement (Table S3), respectively. The resistivity of the copper thin film in the single-pulse $Cu(hfac)_2$ mode is undetected due to high contact resistance (>100 kΩ). Interestingly, the obtained copper thin film with the thickness of ~ 50 nm in the triple-pulse $Cu(hfac)_2$ mode can be as low as 5.6 μΩ·cm, closes to that (2.4 μΩ·cm, 120 nm) reported for the copper thin film grown on SiO_2 substrates by ALD from single-pulse Cu $(hfac)_2$ precursor [16]. The value is still higher than 1.68 μΩ·cm of bulk Cu,[17] which can be attributed to several factors, including surface scattering, grain boundary scattering and the presence of a few zinc impurities in the copper thin film [18].

Surface XPS analysis was used to analyze the adsorption, desorption and molecular conformation of $Cu(hfac)_2$ precursor on the PI substrates in order to determine whether or not $Cu(hfac)_2$ provide valid reaction sites for the efficient adsorption in three different exposure $Cu(hfac)_2$ modes. Fig. 2 shows Cu $2p_{3/2}$ and N 1 s peaks of the $Cu(hfac)_2$-adsorbed surface of treated and untreated PI substrates in single-pulse, dual-pulse

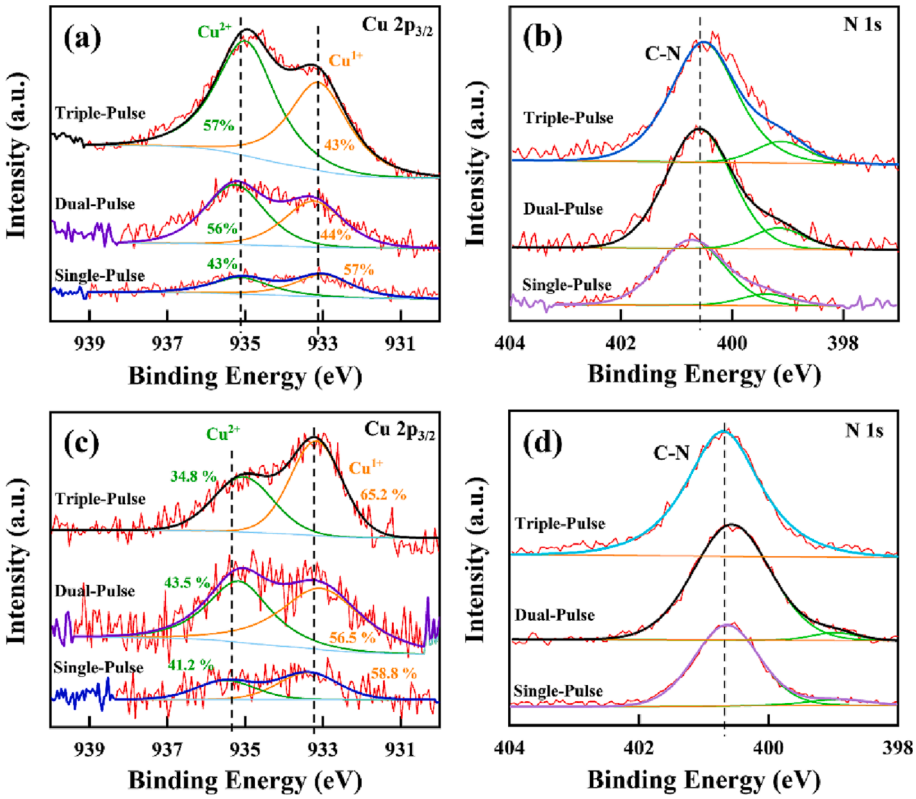

Fig. 2. XPS spectra measured from the surface of $Cu(hfac)_2$-adsorbed treated and untreated PI substrates in single-pulse, dual-pulse and triple-pulse exposure Cu $(hfac)_2$ modes: (a, b) Cu $2p_{3/2}$ peaks and N 1 s peaks on treated PI and (c, d) Cu $2p_{3/2}$ peaks and N 1 s peaks on untreated PI.

and triple-pulse exposure $Cu(hfac)_2$ modes. As Donnelly et al. confirmed, Cu(II) can be partially reduced to Cu(I) for $Cu(hfac)_2$ on TiN (O) surface. [19] In general, the reduction of $Cu(hfac)_2$ can occur through a component that determines whether Cu(I) has been detected. The identification of distinct chemical states of $Cu(hfac)_2$ precursors can be achieved through the calculation of the area ratios associated with each deconvoluted peak. The Cu $2p_{3/2}$ XPS peak of $Cu(hfac)_2$ on the treated polyimide substrate has a typical two-component peak structure located respectively at 933.1–933.3 eV and 933.3–935.5 eV (higher than that of the bulk copper [21]) corresponding to Cu(I) and Cu(II) oxidation states, similar to that of the untreated polyimide substrate. For the surface of $Cu(hfac)_2$-adsorbed PI substrates, the content of Cu(I) in total amount of Cu $2p_{3/2}$ ranges from 43% to 57% and 34.8% to 43.5%, respectively, indicating their physisorption and dissociative chemisorption adsorption. Generally, physisorbed $Cu(hfac)_2$ precursor on conventional smooth Si or glass substrates can be easily removed by the following purging step. In contrast, it is difficult to remove the physisorbed Cu(II)-$(hfac)_2$ on the surface of PI due to its a large porosity and free volume to trap the precursor, resulting in a high content of Cu(II). Furthermore, a comparative experiment on the adsorption of Cu(I) component on the SiO_2 substrate indicates that the proportion of Cu(I) is estimated to be 80% (Figure S4). A distinct difference of Cu(I) adsorption between PI and SiO_2 substrates can be one of the key factors leading to a higher deposition rate (0.079 nm/cycle) of the Cu thin films on the treated PI than that (0.062 nm/cycle) on SiO_2 substrate. The reduction of Cu(II) is considered as a CVD-like parasitic reaction of the ALD-Cu process. It is notable that having a 'CVD' component of growth in a step-wise ALD process does not render it useless, and such processes can show excellent conformality of the deposited film [21]. The utilization of multi-pulse techniques can effectively remove the physisorbed precursor molecules or byproducts on the chemisorbed precursor molecules, leading to improved adsorption efficiency and surface filling rate of the precursor molecules [12]. The data reported here appear to support the assumption that $Cu(hfac)_2$ on treated PI can reach its chemisorption saturation of the reactants for $Cu(hfac)_2$ triple-pulse mode. As shown in Fig. 2a, a significant portion of the adsorbed copper on the polyimide surface exists as physically adsorbed copper precursors, which can be linked to the CVD-like parasitic reaction. It is evident that the ALD-Cu on the polyimide surface is not in the ideal state of perfect self-limiting ALD. Thus, the optimized process of the triple-pulse (3 × 0.5 s) mode is adopted, given the balance between self-limiting ALD and excessive CVD-like parasitic reactions.

As shown in Table S4, a lower average sheet resistance (8.47 Ω/sq) of ALD-Cu thin films (500 growth cycles) on the treated PI substrates for the tripe-pulse mode is obtained than that on the untreated PI (111.77 Ω/sq). The adsorption and nucleation of Cu precursor are enhanced by the pre-treatment process of PI, leading to the improvement of film performance of ALD-Cu. In order to further investigate adsorption amount of $Cu(hfac)_2$ precursors on PI, the XPS peak of imide species (400.9 eV)[22] in the polyimide can be used as a reference peak. Fig. 3a plots the Cu $2p_{3/2}$/N 1 s area ratio as a function of the pulse number of $Cu(hfac)_2$ precursors. An increase of the pulse number seems to lead to an upward trend of Cu content on both untreated and treated polyimides. Moreover, a higher Cu $2p_{3/2}$/N 1 s area ratio of $Cu(hfac)_2$-adsorbed treated PI substrates is obtained compared with that of untreated PI, indicating a higher adsorption capacity of $Cu(hfac)_2$ precursors on the treated polyimide surface. The $Cu(hfac)_2$ precursor is preferentially reacting with the surface carbonyl and hydroxyl groups of polyimides [23,24]. This can be attributed to the increase of active groups on the surface and specific surface area of the treated polyimide than that of the untreated polyimide [25]. Fig. 3b depicts the C 1 s XPS spectra of the PI substrate before and after treatment. Several possible carbon-related components are deconvoluted by curve-fitting the core-level spectra of C1s, including C–C, C-N, C-O, and C = O.[26,27] The bonding extent of C-O and C = O increased from 4.9 % to 12.1 % and 12.8% to 14.9%, respectively. The increase in the C = O and C-O

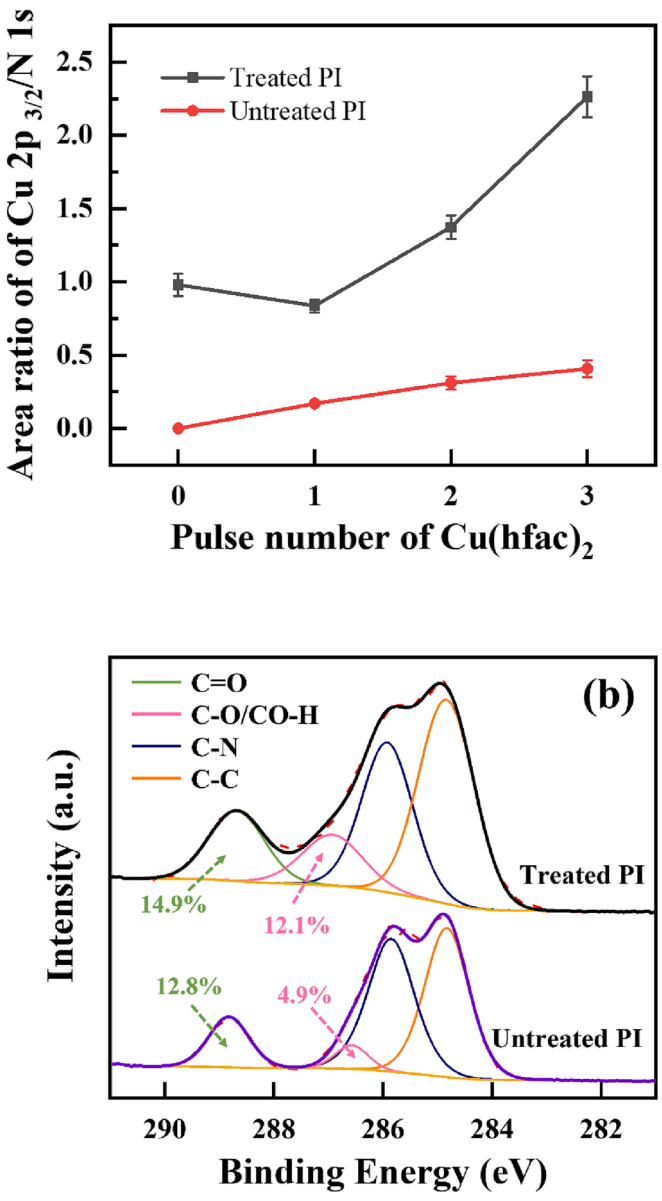

Fig. 3. The XPS survey of the surface of $Cu(hfac)_2$-adsorbed treated and untreated PI substrates: (a) The ratio of XPS peak areas of Cu $2p_{3/2}$/N 1 s as a function of the pulse number of $Cu(hfac)_2$ precursors and (b) C 1 s core-level XPS spectra.

bonding extent can be attributed to the formation of new C-OH and O-C = O bonds resulting from the rupture of C-N-C bonds due to the attack on the symmetric imide rings of PI by hydroxyl group. The pretreatment of NaOH having a ring-opening reaction facilitates the activation of the active sites of PI surface, thereby enabling the incorporation of hydrophilic hydroxyl groups on the surface of PI [28]. AFM images (5.0 × 5.0 μm^2) and contact angle measurement of the treated and untreated polyimide surface are presented in Fig. 4. Comparative measurements on two types of substrates demonstrates that the treated polyimide has a larger root mean square (RMS) roughness (43.0 ± 5 nm) than the untreated polyimide (2.46 ± 0.5 nm). The pre-treated PI surface exhibits numerous micro/nano-scale pores, resulting in a higher roughness (Figure S5). The surface water contact angle is a comprehensive parameter that reflects the physical and chemical properties of a surface influenced by many factors. The findings from these results suggest that surface roughness, substrate surface energy and substrate surface chemical properties can have an effect on water contact angles. It is seen that the water contact angle on the surface of treated polyimide surface is measured to be 62 ± 2°, lower than that (78 ± 2°) on the untreated polyimide substrate. The lower contact angle value suggests an increase in the surface activity and specific surface area of the treated polyimide, which is originated from the creation of new binding states by the treatment process.

In this section, it has been explained that the treated polyimide substrates tend to perform in a triple-pulse mode of $Cu(hfac)_2$ precursor better than the untreated polyimide on evaluation of adsorption of Cu $(hfac)_2$ precursor. The chemical and physical modification of PI enhances the availability of nucleation sites on the PI surface, facilitating the deposition of ALD-Cu precursors and amplifying the overall adsorption area. Analogous to electroless plating on a PI surface, [28] enhancing the roughness and formation of active groups on the PI surface is a basic measure to improve the bond strength and enhance the interaction between the copper and the PI.A schematic of adsorption mechanism of $Cu(hfac)_2$ adsorbed on the surface of the treated polyimide is presented in Fig. 5. On the one hand, $Cu(hfac)_2$ is partially reduced by the hydroxyl groups (–OH, –COOH) of treated surface to form a Cu(I)-hfac. There is one additional hfac ligand protonation to form the volatile H-hfac neutral molecule. [29,30] On the other hand, $Cu(hfac)_2$ is also physisorbed on a PI substrate through dipole–dipole interactions between the precursor and the PI substrate surface [7]. Thus, during the initial growth cycles of ALD-Cu, $Cu(hfac)_2$ precursors with two distinct chemical states on the surface of polyimide can be reduced by Et_2Zn:

$$2Cu(\text{I}) - hfac + Et_2Zn \longrightarrow Zn(hfac)_2 \uparrow + C_4H_{10} \uparrow + 2Cu^0 \quad (1)$$

$$Cu(\text{II}) - (hfac)_2 + Et_2Zn \longrightarrow Zn(hfac)_2 \uparrow + C_4H_{10} \uparrow + Cu^0 \quad (2)$$

3.2. Growth of the copper thin film on the surface of the polyimide

Fig. 6 shows SEM top-view images of the copper thin films deposited on treated polyimide substrates by undergoing 50–500 growth cycles using a triple-pulse mode of $Cu(hfac)_2$ precursor at 120 °C. As shown in Fig. 6a, no obvious copper islands are observed on the surface of the sample after 50 Cu-ALD cycles deposition, similar to that of the treated PI substrate at initial state. Both the treated PI coated and uncoated by ALD-Cu share a number of key features such as loosely-packed nanostructures, as shown in Figure S6. In contrast, the samples with the growth cycles of ≥ 200 possess uniformly distributed copper islands of uniform size, as shown in Fig. 6b, 6c and 6d. Homogeneous copper particles of small size are clearly visible as discontinuous and isolated islands for the sample deposited using 200 ALD growth cycles. As the number of growth cycles increases (300 cycles), the distribution density of copper islands increases noticeably, and the size of individual copper islands does not increase significantly, as presented in Fig. 6c. The copper islands are found to be gradually coalesce and amalgamate to form larger grains for 500 growth cycles, as depicted in Fig. 6d. A continuous copper thin film is achieved on the surface of the polyimide substrates. The production of the continuous copper thin film is critical for obtaining low resistivity (33.45 μΩ·cm) of ALD-Cu on the treated PI surface in the process of the triple-pulse mode and 500 growth cycles. In terms of conventional substrates such as Si, SiO_2, TaN or carbon-doped oxide (COD), the initial formation of Cu islands can occur after only a few growth cycles [6,31,32]. In our case, there are evident incubation cycles and nucleation delays, similar with those of ALD-Al_2O_3 thin films on polymers [33].

Fig. 7 displays Cu $2p_{3/2}$ peaks of XPS spectra from the obtained samples by different ALD-Cu growth cycles (50, 200, 300 and 500 cycles). Comparable shifts are noted for the different growth cycles with values from 933.11 to 932.62 eV. The significant shifts in the binding energies can be contributed to an increase in the metallic nature of

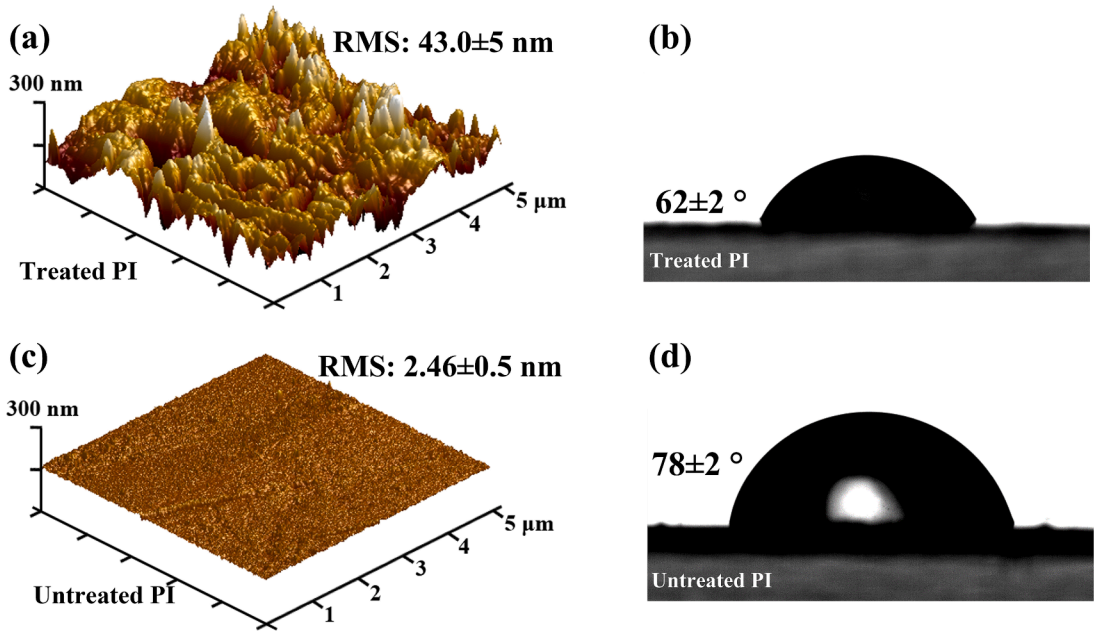

Fig. 4. AFM images (5.0 × 5.0 μm^2) of the surface of (a) treated and (c) untreated PI substrates. Contact angle measurement of the surface of (b) treated and (d) untreated PI substrates.

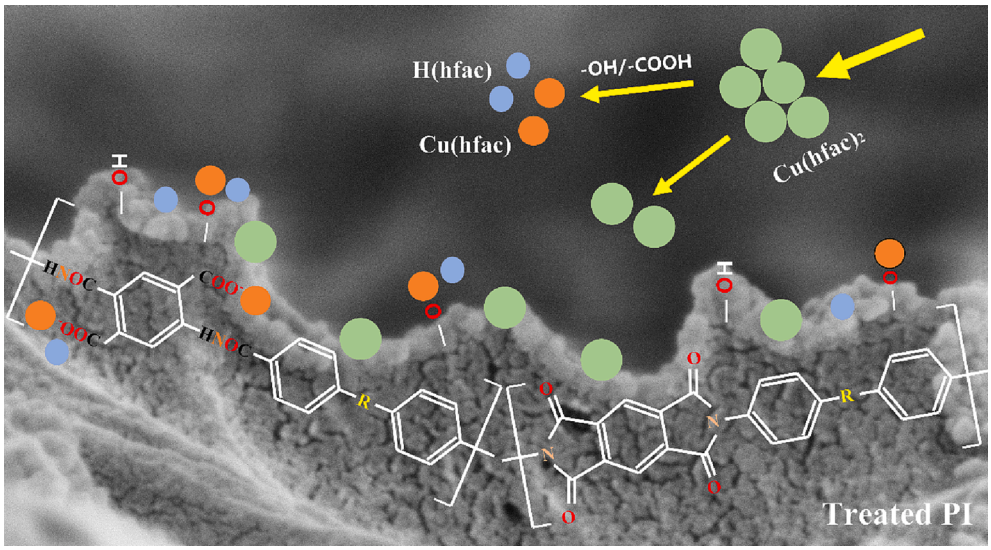

Fig. 5. Proposed adsorption mechanism of Cu(hfac)$_2$ on surface of the treated PI substrates. Cu(II)-(hfac)$_2$, Cu(I)-(hfac) and H-hfac are represented by packed circles of green, orange, and sky blue, respectively. (For interpretation of the references to colour in this figure legend, the reader is referred to the web version of this article.)

copper thin films as increasing the growth cycles of Cu deposition, indicating that the relative interaction at the interface of PI substrates is relatively weak as the Cu thin films grow [27]. Furthermore, the Cu $2p_{3/2}$ peak of the ALD-Cu thin film with over 300 growth cycles is located at ~ 932.62 eV, near to that of bulk copper, suggesting that the surface of polyimide substrate is completely covered by continuous and conformal copper layer. The transition of the ALD-Cu layer from non-continuous to continuous also leads to a maximum (at 300 cycles) of the major peak with increasing growth cycles. In fact, the intensity of XPS peaks is dominated by intrinsic properties of the sample such as surface roughness, grain boundaries, and conductivity. To gain deeper insights into the interaction between ALD-Cu and treated PI substrates, the microstructures and elemental composition across the Cu (1000 growth cycles)/treated PI interface is investigated by TEM equipped with EDX capabilities (Fig. 8). Fig. 8a exhibits a cross-sectional ADF-STEM image of the Cu/PI interface, along with the EDX elemental distribution maps. The signal profile of Cu and C (the primary components of PI) suggests a lack of a well-defined demarcation at the Cu/PI interface, instead exhibiting a prominent composite region. Fig. 8b presents the EDX vertical averaged intensity distribution spectrum corresponding to the ADF-STEM image. The Cu EDX intensity spectra reveals a thickness distribution range of over 100 nm for Cu, with a significant presence in the near-surface region of the treated PI (highlighted in pink). The Cu signal reaches a maximum on the treated PI surface and then decreases gradually across the Cu/PI composite region and finally returns to baseline at a distance of approximately 50 nm from the PI surface. Generally, the presence of impurities in an ALD process are attributed to incomplete purging of unreacted precursors, reaction by-products, or

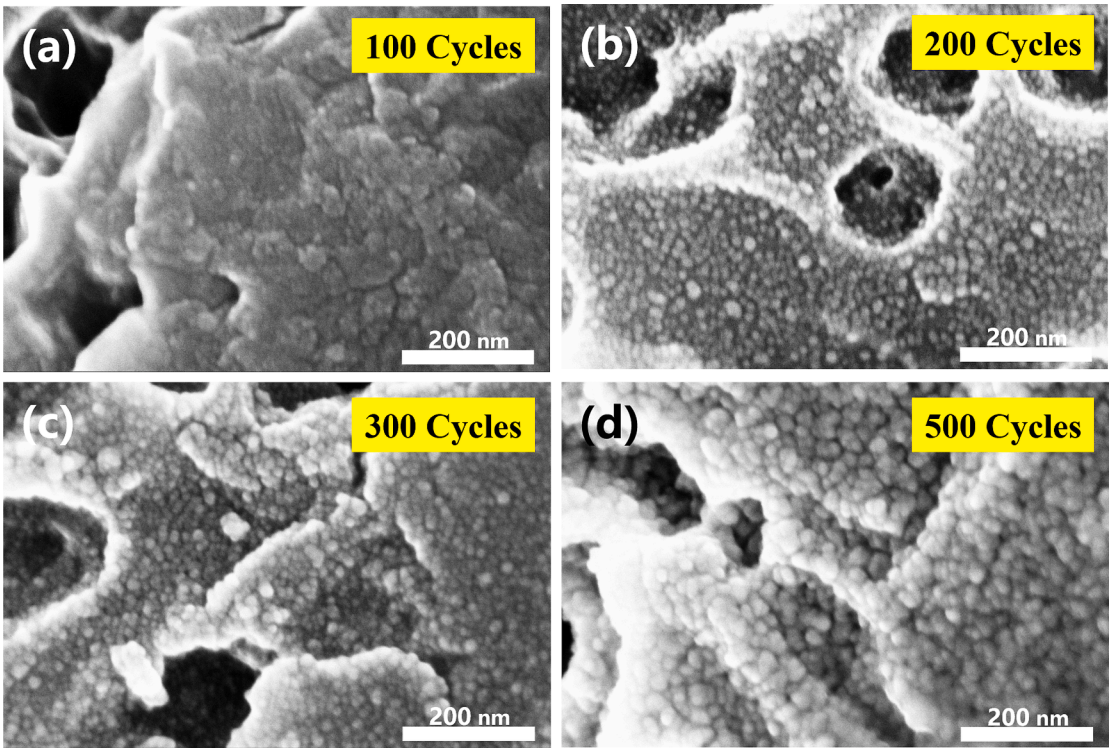

Fig. 6. Comparison of the SEM top-view images of the copper thin films grown on treated PI substrates using (a) 50, (b) 200, (c) 300 and (d) 500 growth cycles.

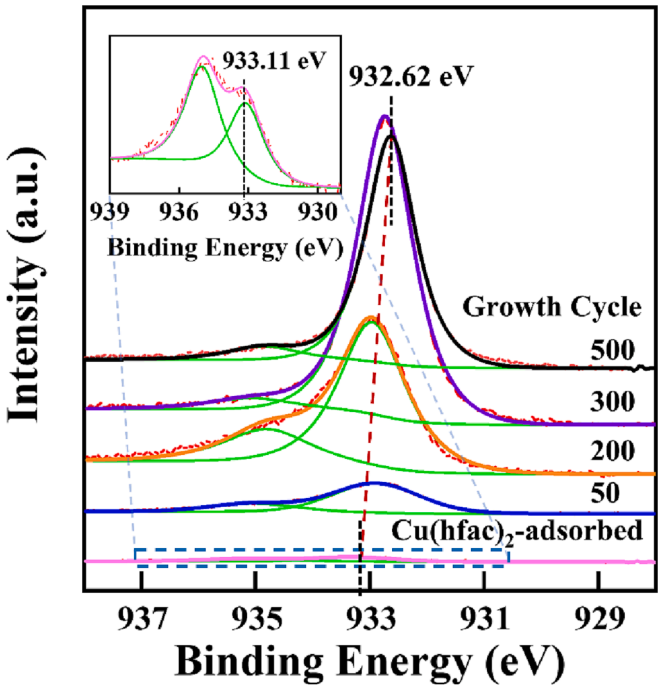

Fig. 7. Cu $2p_{3/2}$ XPS spectra of the copper thin films grown with different ALD growth cycles on treated PI substrates.

decomposed precursors during the deposition process. In this case, the use of Et_2Zn and $Cu(hfac)_2$ precursors (Figure S7) leads to the incorporation of Zn and F impurities in the copper film [19,32]. The enlarged EDX spectrum (Fig. 8e) of Zn and F elements exhibits a distribution range that aligns with the Cu signal, further confirming the presence of a composite layer of approximately 50 nm between ALD-Cu and the treated PI. Those EDX mapping suggests that the precursor has penetrated the near-surface region of PI and react on the PI surface and near-surface area. The cross-sectional low-resolution BF-TEM image (Fig. 8c) of the Cu/PI interface demonstrates a continuously and conformally deposited Cu thin film with a thickness of approximately 48.19 nm on the rough surface of the PI. Furthermore, in the bright-field mode, no distinct Cu/PI boundary is observed. A cross-sectional BF-TEM image of the Cu/PI interface shows a rough polymer/inorganic interface after coating using $Cu(hfac)_2/Et_2Zn$ ALD. Repeated ALD cycles result in near-surface particles along with swelling and roughening of the substrate [34]. These observations are consistent with the results obtained from cross-sectional SEM image (Figure S8) and EDX analysis. The high-resolution transmission electron microscopy (HRTEM) image illustrates the nanoscale crystal structure of the material at the Cu/PI interface, as shown in Fig. 8d. The inverse Fast Fourier Transform (FFT) method based on Digital Micrograph has been utilized to filter the square areas 1 (copper film, blue) and 2 (Cu/PI composite region, orange). Pair of bright spots corresponding to the (1 1 1) planes of Cu can be observed in the related FFT image, indicating that the crystal orientation of ALD-Cu thin film formed on treated PI is predominantly (1 1 1) (Similar to the XRD analysis results of ALD-Cu with 1000 growth cycles on glass substrate shown in Figure S9).) No significant lattice distortion or intermediate phase is observed in the Cu at the composite interface. Overall, based on the distribution of the elements and the morphology of the ALD-Cu/PI interface, the evidence suggests that the ALD-Cu infiltrates the near-surface region of PI through precursor diffusion, adsorption and nucleation. This phenomenon exhibits similarities to the conventional Cu/PI interface [35], but the saturation growth characteristics of ALD lead to complete filling of the molecular chain voids in the near-surface region of PI with copper clusters. The presence of a composite interface indicates that a stronger mechanical interlocking structure has formed at the interface between ALD-Cu and treated PI. This structure is believed to enhance the adhesion between the Cu/PI interface.

A possible growth mechanism of copper thin films on polyimide substrates by low-temperature atomic layer deposition has been proposed based on surface and interface characteristic analysis of Cu and PI,

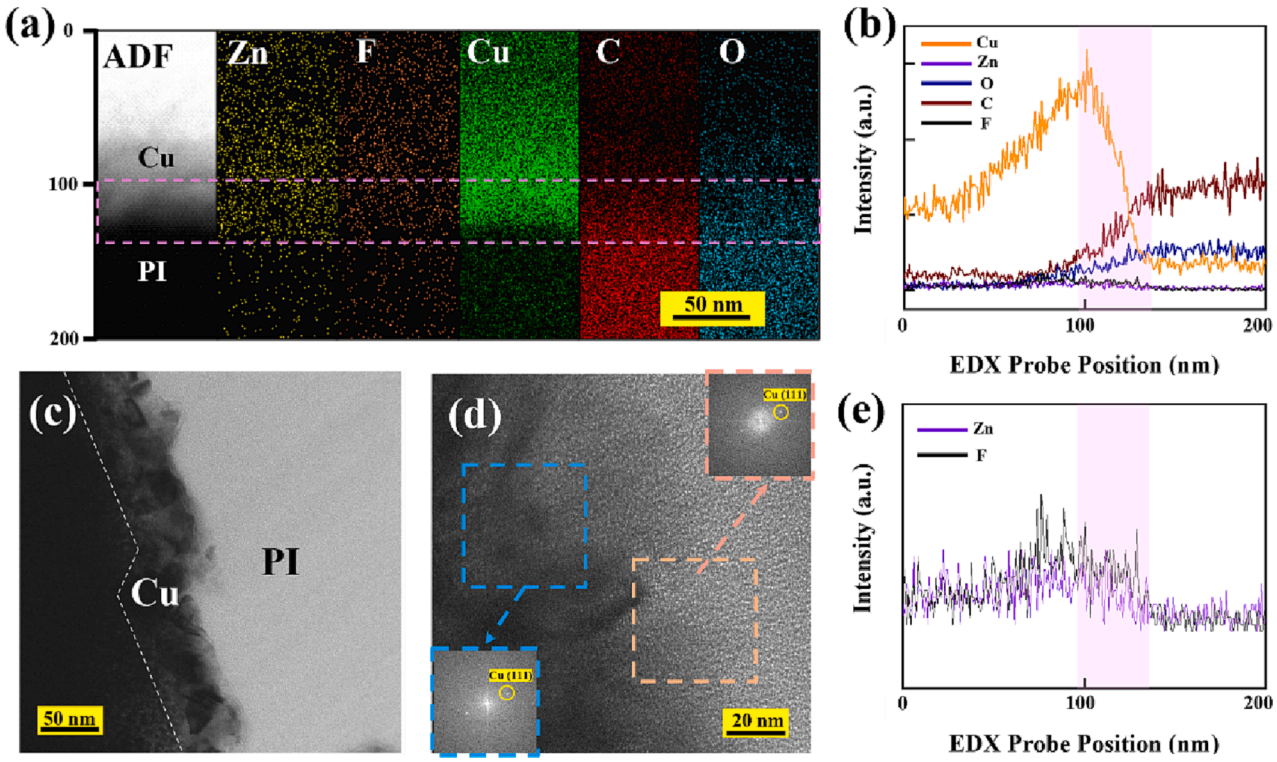

Fig. 8. Characterizations of the Cu (1000 growth cycles)/PI interface. (a) The ADF-STEM image and STEM-EDX elemental maps (Zn, F, Cu, C and O) for the cross-section of the Cu/PI structure. (b, e) Vertically averaged intensity profiles of Zn, F, Cu, C and O across the interface of Cu/PI. The spectra of Zn and F are shown in enlarged plots (e). Note that the horizontal axis is corresponds to the vertical axis of Fig. 8a. (c) Low-magnification cross-sectional BF-TEM image of the Cu/PI interface. (d) The high-resolution TEM (HRTEM) image of the Cu/PI interface, along with FFT patterns (inset) of region 1 (blue), region 2 (Orange). (For interpretation of the references to colour in this figure legend, the reader is referred to the web version of this article.)

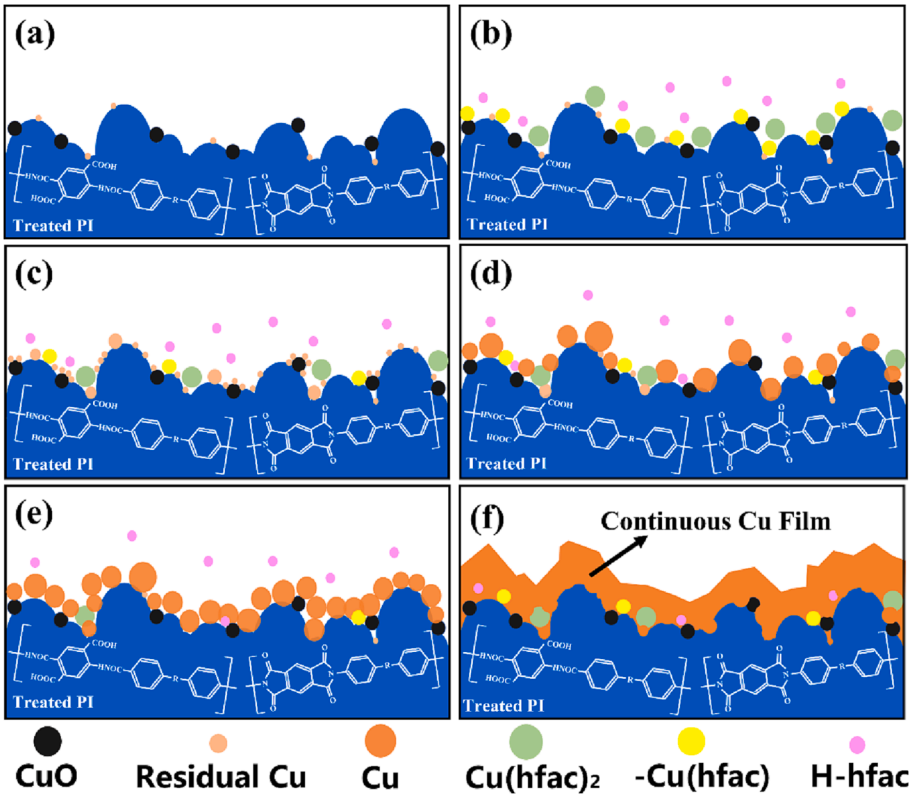

Fig. 9. Proposed nucleation and growth model for ALD-Cu on treated PI showing (a) cross section of treated PI with trace amounts of residual copper and copper oxide, (b) adsorption of copper precursor on near surface region of PI, (c) formation of copper nuclear clusters, (d, e) coalescence and increases of copper islands, and (f) formation of dense, continuous copper film on treated PI surface.

as shown in Fig. 9. The evidence presented thus far supports the idea that can be supported by the XPS analysis of the PI surface and $Cu(hfac)_2$-adsorbed PI surface, cross-sectional and surface SEM of different growth cycles of the ALD copper films, cross-sectional TEM and EDX analyses of the interface of Cu/PI. The deposition of ALD-Cu thin film involves such steps as adsorption and diffusion of reactants, formation of copper islands, growth and coalescence of copper islands (or grains), and finally contributes to a continuous copper thin film. The $Cu(hfac)_2$ precursors and its dissociation products can be adsorbed and trapped in the near-surface region of the polyimide substrates by physisorbtion and chemisorption, as shown in Fig. 9b. Exposed to subsequent Et_2Zn, both $Cu(hfac)_2$, Cu(hfac) and H-hfac can be reduced, and consequently nucleation clusters of copper can be formed, the deposition of ALD-Cu begins from the near-surface region of the PI substrates, as shown in Fig. 9c. As the number of ALD-Cu (atomic layer deposited Cu) growth cycle increases, coalescence of smaller copper islands can be formed on the surface of the polyimide after filling the space between the polymer chains, as illustrated in Fig. 9d. Consequently, the distribution density of copper islands increases with the increase of the number of ALD-Cu growth cycles (Fig. 9e). Finally, a conformal and continuous thin film is formed and completely coated on the surface of the polyimide substrates, as copper islands (copper grains) grow and coalesce with each other, as displayed in Fig. 9f. In fact, the growth rate of ALD-Cu thin films on treated polyimide substrates from 500 to 1000 growth cycles is estimated to be 0.045 nm/cycle, close to that (0.041 nm/cycle) on SiO_2 substrates. One possible implication of this that there exists a stable growth pattern for the surface of continuously grown copper layer. The findings indicate that the growth of ALD-Cu thin films on polyimide substrates can pave an easy path for flexible printed circuits.

4. Conclusions

In summary, copper seed layers are extremely challenging to deposit by atomic layer deposition on polyimide substrates due to the lack of surface polarity and reactivity. In this work, we develop and implement a low-temperature copper atomic layer deposition process, utilizing alternating deposition cycles of a continuous $Cu(hfac)_2$ multi-pulse and Et_2Zn on a treated polyimide surface. Conformal and continuous Cu thin film growth occurred with a growth per cycle of 0.79 Å on a treated polyimide substrates at 120 °C. A ~ 50 nm thickness Cu thin film shows promising resistivities as low as 5.6 μΩ·cm, competitive with bulk Cu. The interaction between $Cu(hfac)_2$ and PI surface during the initial stage of the growth cycle is a key factor affecting the performance of the film. A possible nucleation and growth model of ALD-Cu on polyimide is proposed based on the chemisorption and physisorption of $Cu(hfac)_2$ onto the surface and into the near-surface region of the polyimide. The $Cu(hfac)_2$ is trapped in the near-surface region of the substrates with the presence of Cu(I) and Cu(II) species. This model further elucidates the low-temperature atomic layer deposition mechanism of the copper thin films on polyimide and paves the way for the understanding and optimization of the ALD-Cu on polymeric substrates in present and future studies.

CRediT authorship contribution statement

Zihong Gao: Writing – original draft, Validation, Visualization, Software, Methodology, Investigation, Data curation. **Chengli Zhang:** Funding acquisition, Project administration. **Junhua Gao:** Methodology, Investigation. **Qiang Wang:** Data curation, Visualization, Investigation. **Guanglong Xu:** Data curation, Visualization, Investigation. **Hongtao Cao:** Funding acquisition, Resources, Supervision, Project administration. **Hongliang Zhang:** Funding acquisition, Methodology, Project administration, Resources, Supervision, Writing – review & editing.

Declaration of Competing Interest

The authors declare that they have no known competing financial interests or personal relationships that could have appeared to influence the work reported in this paper.

Data availability

No data was used for the research described in the article.

Acknowledgements

This project is supported by the Ningbo Science and Technology Innovation 2025 Major Special Project (2020Z002).

Appendix A. Supplementary data

Supplementary data to this article can be found online at https://doi.org/10.1016/j.apsusc.2023.158072.

References

[1] S.Q. Hong, C.M. Liu, S.Q. Hao, W.X. Fu, J. Peng, B.H. Wu, N.F. Zheng, Antioxidant High-Conductivity Copper Paste for Low-Cost Flexible Printed Electronics, npj Flex Electron. 6 (1) (2022) 17, https://doi.org/10.1038/s41528-022-00151-1.
[2] J.P. Liu, C. Yang, P.C. Zou, R. Yang, C. Xu, B.H. Xie, Z.Y. Lin, F.Y. Kang, C.P. Wong, Flexible Copper Wires Through Galvanic Replacement of Zinc Paste: A Highly Cost-Effective Technology for Wiring Flexible Printed Circuits, J. Mater. Chem. C 3 (32) (2015) 8329–8335, https://doi.org/10.1039/c5tc01421b.
[3] Y.B. Zhang, T. Zhang, H.B. Shi, Q. Liu, Y.L. Shi, T. Wang, Electroless Plating Cycle Process for High-Conductivity Flexible Printed Circuits, ACS Sustain. Chem. Eng. 9 (35) (2021) 11991–12004, https://doi.org/10.1021/acssuschemeng.1c04613.
[4] J. Lee, J. Yoon, H.G. Kim, S. Kang, W.S. Oh, H. Algadi, S. Al-Sayari, B. Shong, S. H. Kim, H. Kim, T. Lee, H.B.R. Lee, Highly conductive and flexible fiber for textile electronics obtained by extremely low-temperature atomic layer deposition of Pt, NPG Asia Mater. 8 (2016), https://doi.org/10.1038/am.2016.182.
[5] K. Vayrynen, K. Mizohata, J. Raisanen, D. Peeters, A. Devi, M. Ritala, M. Leskela, Low-Temperature Atomic Layer Deposition of Low-Resistivity Copper Thin Films Using $Cu(dmap)_2$ and Tertiary Butyl Hydrazine, Chem. Mater. 29 (15) (2017) 6502–6510, https://doi.org/10.1021/acs.chemmater.7b02098.
[6] Z. Guo, H. Li, Q. Chen, L. Sang, L. Yang, Z. Liu, X. Wang, Low-Temperature Atomic Layer Deposition of High Purity, Smooth, Low Resistivity Copper Films by Using Amidinate Precursor and Hydrogen Plasma, Chem. Mater. 27 (17) (2015) 5988–5996, https://doi.org/10.1021/acs.chemmater.5b02137.
[7] B.H. Lee, J.K. Hwang, J.W. Nam, S.U. Lee, J.T. Kim, S.M. Koo, A. Baunemann, R. A. Fischer, M.M. Sung, Low-Temperature Atomic Layer Deposition of Copper Metal Thin Films: Self-Limiting Surface Reaction of Copper Dimethylamino-2-propoxide with Diethylzinc, Angew. Chem. Int. Ed. 48 (25) (2009) 4536–4539, https://doi.org/10.1002/anie.200900414.
[8] P.P. Xiong, Y.F. Liu, T. Ding, P. Chen, H.R. Wang, Y. Duan, Transparent Electrodes Based on Ultrathin/Ultra Smooth Cu Films Produced Through Atomic Layer Deposition as New ITO-Free Organic Light-Emitting Devices, Org. Electron. 58 (2018) 18–24, https://doi.org/10.1016/j.orgel.2018.03.036.
[9] B.I. Noh, J.W. Yoon, S.B. Jung, Fabrication and Adhesion Strength of Cu/Ni-Cr/polyimide Films for Flexible Printed Circuits, Microelectron. Eng. 88 (6) (2011) 1024–1027, https://doi.org/10.1016/j.mee.2011.01.071.
[10] X.W. Cao, J.W. Wen, C. Wei, X. Liu, G.J. He, Preparation and properties of adhesive-free double-sided flexible copper clad laminate with outstanding adhesion strength, High Perform. Polym. 33 (6) (2021) 704–711, https://doi.org/10.1177/0954008320988761.
[11] A. Konar, K.W. Shin, K.E. Byun, P.P. Shinde, S.P. Adiga, K.S. Mayya, Y. Cho, H. J. Shin, S. Park, Surface Roughness Mediated Specularity Parameter of Thin Cu Films, Appl. Phys. Lett. 118 (13) (2021), https://doi.org/10.1063/5.0038887.
[12] J.C. Park, C.I. Choi, S.G. Lee, S.J. Yoo, J.H. Lee, J.H. Jang, W.H. Kim, J.H. Ahn, J. H. Kim, T.J. Park, Advanced Atomic Layer Deposition: Metal Oxide Thin Film Growth Using the Discrete Feeding Method, J. Mater. Chem. C 11 (4) (2023) 1298–1303, https://doi.org/10.1039/d2tc03485a.
[13] S.-W. Kang, J.-Y. Yun, Y.H. Chang, Growth of Cu Metal Films at Room Temperature Using Catalyzed Reactions, Chem. Mater. 22 (5) (2010) 1607–1609, https://doi.org/10.1021/cm902294e.
[14] C. Jezewski, W.A. Lanford, C.J. Wiegand, J.P. Singh, P.I. Wang, J.J. Senkevich, T. M. Lu, Inductively Coupled Hydrogen Plasma-Assisted Cu ALD on Metallic and Dielectric Surfaces, J. Electrochem. Soc. 152 (2) (2005) C60–C64, https://doi.org/10.1149/1.1850340.
[15] V.H. Nguyen, A. Sekkat, C. Jimenez, D. Munoz, D. Bellet, D. Munoz-Rojas, Impact of Precursor Exposure on Process Efficiency and Film Properties in Spatial Atomic Layer Deposition, Chem. Eng. J. 403 (2021), https://doi.org/10.1016/j.cej.2020.126234.

[16] R. Solanki, B. Pathangey, Atomic Layer Deposition of Copper Seed Layers, Electrochemical and Solid State Letters 3 (10) (2000) 479–480, https://doi.org/10.1149/1.1391185.
[17] H.D. Liu, Y.P. Zhao, G. Ramanath, S.P. Murarka, G.C. Wang, Thickness Dependent Electrical resistivity of Ultrathin (< 40 nm) Cu Films, Thin Solid Films 384 (1) (2001) 151–156, https://doi.org/10.1016/s0040-6090(00)01818-6.
[18] M. Shimada, M. Moriyama, K. Ito, S. Tsukimoto, M. Murakami, Electrical Resistivity of Polycrystalline Cu Interconnects with Nano-Scale Linewidth, J. Vac. Sci. Technol. B 24 (1) (2006) 190–194, https://doi.org/10.1116/1.2151910.
[19] V.M. Donnelly, M.E. Gross, Copper Metalorganic Chemical Vapor Deposition Reactions of Hexafluoroacetylacetonate Cu(I) vinyltrimethylsilane and Bis (hexafluoroacetylacetonate) Cu(II) Adsorbed on Titanium Nitride, J. Vac. Sci. Technol. A 11 (1) (1993) 66–77, https://doi.org/10.1116/1.578721.
[20] C.D. Wagner, W.M. Riggs, L.E. Davis, J.F. Moulder, G.E. Muilenberg, Handbook of X-ray Photoelectron Spectroscopy, Perkin-Elmer Corporation, Eden Prairie, Minn, 1992, p. 203.
[21] P.G. Gordon, A. Kurek, S.T. Barry, Trends in Copper Precursor Development for CVD and ALD Applications, ECS J. Solid State Sci. Technol. 4 (1) (2014) N3188–N3197, https://doi.org/10.1149/2.0261501jss.
[22] L.P. Buchwalter, X-ray Photoelectron Spectroscopy and Infrared Spectroscopy Analysis of Pyromellitic Dianhydride-Oxydianiline Polyamide-Acid and Polyamide-Ester Imidization, J. Vac. Sci. Technol. A 7 (3) (1989) 1772–1777, https://doi.org/10.1116/1.576044.
[23] N.L. Jeon, R.G. Nuzzo, Physical and Spectroscopic Studies of the Nucleation and Growth of Copper Thin Films on Polyimide Surfaces by Chemical Vapor Deposition, Langmuir 11 (1) (1995) 341–355, https://doi.org/10.1021/la00001a057.
[24] P. Martensson, J.O. Carlsson, Atomic Layer Epitaxy of Copper-Growth and Selectivity in the Cu(II)-2,2,6,6-tetramethyl-3,5-heptanedionate/H-2 Process, J. Electrochem. Soc. 145 (8) (1998) 2926–2931, https://doi.org/10.1149/1.1838738.
[25] J.H. Kim, Y.G. Seol, N.E. Lee, Adhesion Properties of Electroless-Plated Cu Layers on Polyimide Treated by Inductively Coupled Plasmas, J. Korean Phys. Soc. 51 (2007) S187–S192, https://doi.org/10.3938/jkps.51.187.
[26] S.H. Kim, S.W. Na, N.E. Lee, Y.W. Nam, Y.H. Kim, Effect of Surface Roughness on the Adhesion Properties of Cu/Cr Films on Polyimide Substrate Treated by Inductively Coupled Oxygen Plasma, Surf. Coat. Technol. 200 (7) (2005) 2072–2079, https://doi.org/10.1016/j.surfcoat.2005.05.021.
[27] S. Pimanpang, P.-I. Wang, J.S. Juneja, G.C. Wang, T.M. Lu, Interfacial Interaction of In Situ Cu Growth on Tetrasulfide Self-Assembled Monolayer on Plasma Treated Parylene Surface, J. Vac. Sci. Technol. A 24 (5) (2006) 1884–1891, https://doi.org/10.1116/1.2333574.
[28] W.X. Yu, L. Hong, B.H. Chen, T.M. Ko, A Study on the Interfacial Composition of the Electroless Copper Plated BPDA-PDA Polyimide Sheet, J. Mater. Chem. 13 (4) (2003) 818–824, https://doi.org/10.1039/b208102d.
[29] S. Pimanpang, P.I. Wang, D. Ye, J.S. Juneja, G.C. Wang, T.M. Lu, Enhancement of $Cu(hfac)_2$ Chemisorption on the Parylene Surface by N_2 Plasma Surface Modification, J. Electrochem. Soc. 154 (10) (2007) G215–G219, https://doi.org/10.1149/1.2766606.
[30] S.L. Cohen, M. Liehr, S. Kasi, Mechanisms of Copper Chemical Vapor Deposition, Appl. Phys. Lett. 60 (1) (1992) 50–52, https://doi.org/10.1063/1.107370.
[31] D.J. Hagen, J. Connolly, I.M. Povey, S. Rushworth, M.E. Pemble, Island Coalescence during Film Growth: An Underestimated Limitation of Cu ALD, Adv. Mater. Interfaces 4 (18) (2017) 1700274, https://doi.org/10.1002/admi.201700274.
[32] Z.Y. Zhong, X.Q. Wang, J.N. Ding, N.Y. Yuan, Nanometer-Thick Copper Films Grown by Thermal Atomic Layer Deposition, Thin Solid Films 589 (2015) 673–680, https://doi.org/10.1016/j.tsf.2015.06.053.
[33] C.A. Wilson, R.K. Grubbs, S.M. George, Nucleation and Growth During Al_2O_3 Atomic Layer Deposition on Polymers, Chem. Mater. 17 (23) (2005) 5625–5634, https://doi.org/10.1021/cm050704d.
[34] H.C. Guo, E.Y. Ye, Z.B. Li, M.Y. Han, X.J. Loh, Recent progress of atomic layer deposition on polymeric materials, Materials Science and Engineering C-Materials for Biological Applications 70 (2017) 1182–1191, https://doi.org/10.1016/j.msec.2016.01.093.
[35] R.M. Tromp, F. Legoues, P.S. Ho, Interdiffusion at the Polyimide-Cu Interface, J. Vac. Sci. Technol. A 3 (3) (1985) 782–785, https://doi.org/10.1116/1.573308.